



UNIVERSITY OF LEEDS

This is a repository copy of *Ultra Fast Linear State Estimation Utilizing SCADA Measurements*.

White Rose Research Online URL for this paper:
<http://eprints.whiterose.ac.uk/142961/>

Version: Accepted Version

Article:

Salehi Dobakhshari, A, Azizi, S orcid.org/0000-0002-9274-1177, Paolone, M et al. (1 more author) (2019) Ultra Fast Linear State Estimation Utilizing SCADA Measurements. IEEE Transactions on Power Systems, 34 (4). pp. 2622-2631. ISSN 0885-8950

<https://doi.org/10.1109/TPWRS.2019.2894518>

(c) 2018 IEEE. Personal use of this material is permitted. Permission from IEEE must be obtained for all other uses, in any current or future media, including reprinting/republishing this material for advertising or promotional purposes, creating new collective works, for resale or redistribution to servers or lists, or reuse of any copyrighted component of this work in other works.

Reuse

Items deposited in White Rose Research Online are protected by copyright, with all rights reserved unless indicated otherwise. They may be downloaded and/or printed for private study, or other acts as permitted by national copyright laws. The publisher or other rights holders may allow further reproduction and re-use of the full text version. This is indicated by the licence information on the White Rose Research Online record for the item.

Takedown

If you consider content in White Rose Research Online to be in breach of UK law, please notify us by emailing eprints@whiterose.ac.uk including the URL of the record and the reason for the withdrawal request.



eprints@whiterose.ac.uk
<https://eprints.whiterose.ac.uk/>

Ultra Fast Linear State Estimation Utilizing SCADA Measurements

A. Salehi Dobakhshari, *Member, IEEE*, S. Azizi, *Member, IEEE*, M. Paolone, *Senior Member, IEEE*, and V. Terzija, *Fellow, IEEE*

Abstract—This paper presents a closed-form and non-iterative solution for the long-studied SCADA-based State Estimation (SE) problem, where unsynchronized traditional measurements from Remote Terminal Units (RTUs) are used. In this regard, a novel reformulation of the problem is introduced where unknowns are expressed as complex variables in terms of unsynchronized SCADA measurements. To this end, it is assumed that bus voltage amplitudes as well as current amplitudes and active and reactive power flows/injections are available. The resulting system of equations is solved by the classic linear weighted least-squares method. In contrast to the traditional approaches, several drawbacks such as initialization and issues with convergence (especially for large-scale systems) are resolved. Moreover, the proposed approach does not use synchrophasors. The method is validated on a 3-bus test network and applied to the IEEE 118-bus test system, 1341-bus and 9241-bus European high-voltage transmission networks.

Index Terms—Complex analysis, Linear least-squares estimation, Power system operation, RTU, SCADA, State estimation, Unsynchronized measurements.

I. NOMENCLATURE

E_a	True voltage amplitude at bus a .
E_a^{meas}	Voltage amplitude measurement at bus a .
\mathbf{E}_a	Unknown complex voltage at bus a with respect to the reference bus.
I_{ab}	True current amplitude through line a - b .
θ_{ab}	True phase angle of the current through line a - b (with respect to \mathbf{E}_a).
I_{ab}^{meas}	Current amplitude measurement through line a - b measured at bus a .
θ_{ab}^{meas}	Measured/Calculated phase-angle of the current through line a - b (with respect to \mathbf{E}_a).
I_{ab}^{local}	True complex current through line a - b (with respect to \mathbf{E}_a).
\mathbf{I}_{ab}	Unknown complex current through line a - b with respect to the reference bus at bus a .
$I_{a,inj}^{local}$	True complex current injection (with respect to \mathbf{E}_a) at bus a .

$I_{a,inj}$	True complex current injection at bus a with respect to the reference bus.
P_{ab}, Q_{ab}	True active and reactive power flows through line a - b on terminal a .
e_{E_a}	Amplitude measurement error of E_a^{meas} .
$e_{I_{ab}}$	Amplitude measurement error of I_{ab}^{meas} .
$e_{\theta_{ab}}$	Angle measurement/calculation error of θ_{ab}^{meas} .
δ_a	Unknown phase angle of complex voltage at bus a with respect to the slack bus voltage phasor.
Z_{ab}	Series impedance of transmission line a - b .
Y_{ab}	Shunt admittance of transmission line a - b .
H	Known matrix of the measurement model used to formulate the SE problem.
m	Number of measurements.
n	Number of buses.

II. INTRODUCTION

POWER system state estimation is an essential prerequisite for secure and economic power system operation [1]. Conventionally, the Supervisory Control And Data Acquisition (SCADA) system utilizing RTUs in substations provides busbar voltage amplitudes as well as currents and active and reactive powers flowing through transmission lines or injected into busbars. The advantages of using non-synchronized SCADA-based measurements are the utilization of existing infrastructure and exploiting redundant measurements. These measurements, however, are nonlinearly related to the system state variables, composed of the phasors of nodal voltages [2]. In order to solve this problem, iterative methods based on the Gauss-Newton algorithms are usually adopted [3]. Although this solution is widely adopted in real-world situational awareness systems [4], it still suffers from inherent problems associated with iterative algorithms, i.e., failure of the algorithm to converge, the speed of convergence, and concerns over multiplicity of the solution and sensitivity to initial values chosen for the system states.

To address these difficulties, convexification of power flow equations through semidefinite and conic programming has recently attracted attention [5]–[9]. Although this approach has shown promising results for power system SE, the convexification of the problem may not yield a feasible solution, and the algorithm yet remains iterative. Other approaches use factorized [10] and bilinear [11]–[13] formulations of the SE.

A. Salehi Dobakhshari is with the Faculty of Engineering, University of Guilan, Rasht 4199613776, Iran (e-mail: salehi_ahmad@guilan.ac.ir).

S. Azizi and V. Terzija are with the School of Electrical and Electronic Engineering, The University of Manchester, Manchester M13 9PL, U.K. (e-mail: sadegh.azizi@manchester.ac.uk; vladimir.terzija@manchester.ac.uk).

M. Paolone is with the École Polytechnique Fédérale de Lausanne, Lausanne CH-1015, Switzerland (e-mail: mario.paolone@epfl.ch).

However, also these formulations rely on nonlinear transformations, which need iterations to converge, if an optimal estimate is desired. Linear measurement functions have been developed in [14], which models SE as a constrained linear programming problem with nonlinear constraints and solves it iteratively by interior-point methods.

Direct non-iterative SE methods are mainly focused on utilizing synchrophasor measurements by Phasor Measurement Units (PMUs) [15]–[20]. If the power system is observable by PMUs with sufficient redundancy, then the PMU-only SE [20] can be performed. Otherwise, either SCADA-based or hybrid SCADA/PMU-based state estimation should be used (e.g. [21]–[23]).

Only a few attempts have been made to solve the SE using purely SCADA-based measurements, in a non-iterative manner. The most recent research works include a novel reformulation of the problem in rectangular form by Fardanesh [24] and its extension by Jiang *et al.* [25], [26]. This reformulation, however, introduces an excessive number of additional state variables due to bilinear terms involving the real and imaginary parts of bus voltages. Moreover, this approach needs sign identification for the complex voltages, among other issues, when retrieving the complex voltages.

This paper presents a novel formulation of the power system SE problem using only traditional unsynchronized SCADA measurements. It does not rely on time synchronization technology and associated PMU measurements. In the new problem formulation both measurement and state variables are represented as complex numbers. As known, the traditional SEs express them as pure real variables. This allows linearization of the problem, in contrast to the traditional solution by Schewppe in 1970 [27] repeatedly practiced since then. Thanks to its low computational complexity, the proposed formulation achieves ultra-fast SE for large-scale power systems.

The state estimation method presented in this paper transforms the SE problem into a system of linear equations, which is solved directly without any need for iterations. The main idea is utilizing complex branch and bus-injection currents instead of active and reactive power flows. This allows to directly utilize linear KVL equations in complex form. This approach is in sharp contrast with conventional expression for active and reactive powers, which are dependent on sine and cosine of phase-angle difference between the two bus voltages of the associated branch.

Salient features of the linear formulation for power system SE in this paper include: 1) no need for PMUs to make the SE problem linear; 2) a direct non-iterative solution to the SE problem, thanks to the linearity of equations; 3) low computational burden as only two square matrices each of the size of the number of network buses need to be inverted; 4) no concern over the convergence as a system of linear equations needs to be solved; 5) fast implementation (due to the above

features) along with utilization of sparsity techniques [28].

III. COMPLEX LINEAR EXPRESSION FOR MEASUREMENTS

There are two families of state estimators: the first one assumes that the rate of change of the system state is slow enough in order to be assumed steady with respect to the measurements [2], [3]; the other family assumes that the above hypothesis does not hold and, therefore, the system state includes also the time derivatives of the state variables [29]. Our state estimator belongs to the static SE category [2], [3]. Although future power systems, dominated by inverter-based generators and FACTS devices, will be characterized by shorter time responses, in such systems the assumption of static SE appears reasonable. For example, the ERCOT system in Texas, USA, includes 11 GW wind capacity while the peak load is 70 GW. In such a system, classical RTUs are used with classical static SEs [30], [31]. The error made in that system by the SE does not exceed 3% even in presence of highly-variable wind power [30]. This implies that classical SE still offers a meaningful solution to assess a static system state even in real systems with high penetration of renewable energy sources.

In this respect, we focus on the problem of determining the system state using measurements that are nowadays available by SCADA. These measurements are provided by RTUs that make use of finite time windows to measure amplitudes of powers, currents and voltages [32], [33]. It is worth noting that over these finite windows, the measurements provided by RTUs refer to a system in permanent sinusoidal static condition. Therefore, our approach assumes the state variables to be statistically associated to RTU measurements.

A. Notations

In this paper, a variable such as voltage or current can be represented by its true value, measured value or estimated value. To distinguish, $(\cdot)^{meas}$ and $(\hat{\cdot})$ denote measured and estimated values, respectively, while true values appear without any superscript. $(\cdot)^{local}$ denotes the complex current, calculated with respect to the phase angle of the corresponding bus voltage. It should be noted that $(\cdot)^{local}$ is not a synchrophasor, but a current phasor whose phase angle can be calculated from the measured active and reactive power flows. All complex-valued scalars, vectors and matrices are printed in bold.

B. Complex Currents

A different formulation of the relation between system states and measurements as a linear system of equations is utilized in this paper. This converts the SE problem into the solution of a system of linear equations, which, as its name implies, does not need to be solved in an iterative manner. We begin with

the complex current through line a - b , which can be expressed as

$$\mathbf{I}_{ab}^{local} \triangleq I_{ab} e^{j\theta_{ab}} \quad (1)$$

where I_{ab} and θ_{ab} are related to the current and phase-angle measurements, respectively, as

$$I_{ab}^{meas} = I_{ab} + e_{I_{ab}} \quad (2)$$

$$\theta_{ab}^{meas} = \theta_{ab} + e_{\theta_{ab}} \quad (3)$$

In (2) it is assumed that current amplitude measurements are available. One reason that they are not used in conventional SE is that they deteriorate the algorithm performance [2]. Our algorithm justifies communicating I_{ab} measurements to control center if they are not already available. If P, Q and E are only transmitted by RTU at substation a , then (29) can be used in the SE code to obtain I_{ab} without directly communicating it. It is worth noting that θ_{ab}^{meas} is the difference between the phase angle of voltage waveform at bus a and that of current waveform along branch a - b . It may be calculated from availability of active and reactive power measurements as

$$\theta_{ab} = \text{tg}^{-1} \left(-\frac{Q_{ab}}{P_{ab}} \right) \quad (4)$$

where P_{ab} and Q_{ab} are the measurable active and reactive power through line a - b (from bus a toward bus b), respectively. The power factors, like all the system state variables, are continuous functions of time. Similar to the any other existing method on static state estimation [2], [3], in which it is assumed that P, Q, E remain constant during the time window when the measurements are taken, we have assumed power factor remains constant as well.

The assumption related to the slow variation of the system state is a prerequisite enabling application of static SEs [2], [3]. All SE functions developed by GE, ABB, Siemens, etc., which are currently in use in worldwide EMSs, are based on the same steady-state assumption as that of this paper [30], [34], [35]. It should be noted that although θ_{ab} can be calculated by P_{ab} and Q_{ab} measurements obtained by the RTU at bus a , this does not mean that δ_a is considered known to the state estimator, as voltages and complex currents measured at different locations, including those measured at bus a , are obviously unsynchronized. This has been demonstrated in Fig. 1. It should be noted that voltage and current phasors have been used regularly in protection relays in absence of telecom infrastructure for many years, as each measurement device can have its own local time reference.

With reference to the slack bus, complex current measurement may be expressed as

$$\mathbf{I}_{ab} = \mathbf{I}_{ab}^{local} e^{j\delta_a} \quad (5)$$

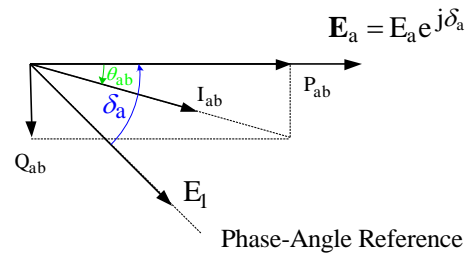


Figure 1. Calculating θ_{ab} by P_{ab} and Q_{ab} while measurements are unsynchronized (δ_a is unknown).

where δ_a is the unknown phase angle of complex voltage at bus a , with reference to the slack bus.¹ It is assumed that system branches can be modeled as passive, reciprocal two-port equivalents and there are no unbalances in the grid [2], [3]. In view of this assumption, any branch of the grid can be modeled as a pi equivalent. We express complex current at bus a through any branch a - b in terms of state variables, which are voltage phasors, as follows.

$$\mathbf{I}_{ab} = (\mathbf{Y}_{ab} + \frac{1}{\mathbf{Z}_{ab}}) \mathbf{E}_a + (-\frac{1}{\mathbf{Z}_{ab}}) \mathbf{E}_b \quad (6)$$

where \mathbf{Y}_{ab} and \mathbf{Z}_{ab} are the transmission line shunt admittance and series impedance, respectively.

1) *Current Flow Measurements:* To express complex current measurement through branch a - b in (1), it is sufficient to substitute (5) into (6) as

$$\mathbf{I}_{ab}^{local} e^{j\delta_a} = (\mathbf{Y}_{ab} + \frac{1}{\mathbf{Z}_{ab}}) \mathbf{E}_a + (-\frac{1}{\mathbf{Z}_{ab}}) \mathbf{E}_b \quad (7)$$

It is worth noting that a different reformulation of the flow measurements is utilized here, in contrast with conventional SE.

2) *Injected Current Measurements:* Consider current injection at bus a . Similar to (6), KCL may be written as

$$\mathbf{I}_{a,inj} = \sum_{b \in L_a} \mathbf{I}_{ab} \quad (8)$$

where L_a is the set of branches connected to bus a . Similar to (7), one can write

$$\mathbf{I}_{a,inj}^{local} e^{j\delta_a} = \sum_{b \in L_a} (\mathbf{Y}_{ab} + \frac{1}{\mathbf{Z}_{ab}}) \mathbf{E}_a + (-\frac{1}{\mathbf{Z}_{ab}}) \mathbf{E}_b \quad (9)$$

where $\mathbf{I}_{a,inj}^{local}$ is the complex current injection measured with respect to the phase angle of voltage at bus a , similar to (1)-(3). Zero-injection is a special case of injection measurement, in which the left hand side of (9) is zero.

¹Note that in traditional RTU-based state estimators, phase-angle reference is needed in view of the absence of an absolute time reference in the measurements. This reference is usually defined as the argument of the fundamental frequency phasor of the voltage waveform of the slack bus.

C. Complex Voltages

As the bus voltage measurements are in fact magnitudes of state variables (complex voltages), it is therefore needed to include phase-angle values for bus voltages as state variables. In this way, bus voltage measurement at any bus is related to the associated complex bus voltage as

$$E_a e^{j\delta_a} = \mathbf{E}_a \quad (10)$$

where E_a is related to the measured voltage amplitude at bus a as

$$E_a^{meas} = E_a + e_{E_a} \quad (11)$$

The phase-angle operator does not appear in (10) for slack bus, whose phase angle is set to zero.

IV. LINEAR ESTIMATION OF VOLTAGE PHASE ANGLES

Equations (7), (9) and (10) show nonlinear relationships between measurements and system states, i.e. bus voltage magnitudes and phase angles. Manipulating these equations will result in a linear reformulation of the problem, if the exponential phase-angle operators, that appear in (7), (9) and (10), are included in the state vector, together with complex voltages.

As such, integrating both voltage and current measurements yields a linear system of equations as shown in (12) at the bottom of next page. The first n rows concern voltage measurements. In addition, current measurements at branches 1-2, 2- n , n -1 and n -2, as well as injection measurement at buses 1 and 2 are demonstrated in this linear system of equations.

In a compact form, (12) can be rewritten as

$$\mathbf{H}\mathbf{x} + \mathbf{e} = \mathbf{z} \quad (13)$$

where \mathbf{H} is of size $m \times (2n - 1)$ and \mathbf{e} is the vector of complex measurement errors (See Appendix A). In both \mathbf{H}

and \mathbf{z} , true variables (See Section III.A) are used in order to save space. From (1)-(3), the relationship between true and measured currents can be deduced. Likewise, for true and measured voltages are related by (10)-(11). If the number of measurements exceeds two times the number of buses minus one, a closed-form solution results from (13) as follows

$$\hat{\mathbf{x}} = (\mathbf{H}^* \mathbf{H})^{-1} \mathbf{H}^* \mathbf{z} \quad (14)$$

where $\hat{\mathbf{x}}$ is the least-squares estimate of \mathbf{x} . Let us partition matrix $(\mathbf{H}^* \mathbf{H})$ and vector $(\mathbf{H}^* \mathbf{z})$ as follows.

$$\mathbf{H}^* \mathbf{H} = \begin{bmatrix} \mathbf{A} & \mathbf{B} \\ \mathbf{C} & \mathbf{D} \end{bmatrix} \quad (15)$$

$$\mathbf{H}^* \mathbf{z} = \begin{bmatrix} \mathbf{z}_1 \\ \mathbf{z}_2 \end{bmatrix} \quad (16)$$

where \mathbf{A} , \mathbf{B} , \mathbf{C} , \mathbf{D} , \mathbf{z}_1 and \mathbf{z}_2 are of size $n \times n$, $n \times (n-1)$, $(n-1) \times n$, $(n-1) \times (n-1)$, $n \times 1$ and $(n-1) \times 1$, respectively. Referring to (12), one can observe that \mathbf{A} and \mathbf{C} only include network parameters. Furthermore, a closer look at the format of \mathbf{H} reveals that the last $(n-1)$ columns of \mathbf{H} have at most one nonzero element at each row, which corresponds to the voltage or current measurement of the associated bus. This property of \mathbf{H} makes \mathbf{D} a real-valued diagonal matrix. In addition, the measurements taken from the first bus appear in \mathbf{z} , while other voltage and current measurements are included in \mathbf{H} . Therefore, all elements of \mathbf{z}_2 are zero. Schur-Banachiewicz inversion formula [36] gives the inverse of $\mathbf{H}^* \mathbf{H}$ as

$$\begin{bmatrix} \mathbf{A} & \mathbf{B} \\ \mathbf{C} & \mathbf{D} \end{bmatrix}^{-1} = \begin{bmatrix} (\mathbf{A} - \mathbf{B}\mathbf{D}^{-1}\mathbf{C})^{-1} & \mathbf{E} \\ -\mathbf{D}^{-1}\mathbf{C}(\mathbf{A} - \mathbf{B}\mathbf{D}^{-1}\mathbf{C})^{-1} & \mathbf{F} \end{bmatrix} \quad (17)$$

where \mathbf{E} and \mathbf{F} are not important here. Substituting (15), (16) and (17) into (14), one can solve for \mathbf{x} as follows.

$$\hat{\mathbf{x}} = \begin{bmatrix} (\mathbf{A} - \mathbf{B}\mathbf{D}^{-1}\mathbf{C})^{-1} \mathbf{z}_1 \\ -\mathbf{D}^{-1}\mathbf{C}(\mathbf{A} - \mathbf{B}\mathbf{D}^{-1}\mathbf{C})^{-1} \mathbf{z}_1 \end{bmatrix} \quad (18)$$

$$\begin{bmatrix} 1 & 0 & \dots & 0 & 0 & 0 & \dots & 0 \\ 0 & -1 & \dots & 0 & E_2 & 0 & \dots & 0 \\ \vdots & \vdots & \vdots & \vdots & \vdots & \vdots & \dots & \vdots \\ 0 & 0 & \dots & -1 & 0 & 0 & \dots & E_n \\ \mathbf{Y}_{12} + \mathbf{Z}_{12}^{-1} & -\mathbf{Z}_{12}^{-1} & 0 & 0 & 0 & 0 & \dots & 0 \\ 0 & \mathbf{Y}_{2n} + \mathbf{Z}_{2n}^{-1} & \dots & -\mathbf{Z}_{2n}^{-1} & -\mathbf{I}_{2n}^{local} & 0 & \dots & 0 \\ \vdots & \vdots & \vdots & \vdots & \vdots & \vdots & \dots & \vdots \\ 0 & -\mathbf{Z}_{n2}^{-1} & 0 & \mathbf{Y}_{n2} + \mathbf{Z}_{n2}^{-1} & 0 & \dots & 0 & -\mathbf{I}_{n2}^{local} \\ -\mathbf{Z}_{n1}^{-1} & 0 & 0 & \mathbf{Y}_{n1} + \mathbf{Z}_{n1}^{-1} & 0 & \dots & 0 & -\mathbf{I}_{n1}^{local} \\ \mathbf{Y}_{12} + \mathbf{Z}_{12}^{-1} + \mathbf{Y}_{1n} + \mathbf{Z}_{1n}^{-1} & -\mathbf{Z}_{12}^{-1} & 0 & -\mathbf{Z}_{1n}^{-1} & 0 & 0 & \dots & 0 \\ -\mathbf{Z}_{21}^{-1} & \mathbf{Y}_{21} + \mathbf{Z}_{21}^{-1} + \mathbf{Y}_{2n} + \mathbf{Z}_{2n}^{-1} & 0 & -\mathbf{Z}_{2n}^{-1} & -\mathbf{I}_{2,n}^{local} & 0 & \dots & 0 \\ \vdots & \vdots & \vdots & \vdots & \vdots & \vdots & \dots & \vdots \end{bmatrix} \begin{bmatrix} \mathbf{E}_1 \\ \mathbf{E}_2 \\ \vdots \\ \mathbf{E}_n \\ e^{j\delta_2} \\ \vdots \\ e^{j\delta_n} \end{bmatrix} = \begin{bmatrix} E_1 \\ 0 \\ \vdots \\ 0 \\ \mathbf{I}_{12}^{local} \\ 0 \\ \vdots \\ 0 \\ 0 \\ \mathbf{I}_{1,inj}^{local} \\ 0 \\ \vdots \end{bmatrix} \quad (12)$$

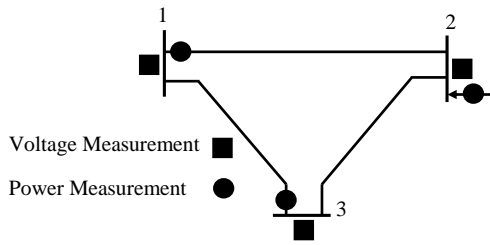


Figure 2. SLD and measurements of a 3-bus network [2].

The phase-angle vector of complex voltages are therefore estimated as

$$\begin{bmatrix} e^{j\hat{\delta}_2} \\ \vdots \\ e^{j\hat{\delta}_n} \end{bmatrix} = -D^{-1}\mathbf{C}(\mathbf{A} - \mathbf{B}D^{-1}\mathbf{C})^{-1}\mathbf{z}_1 \quad (19)$$

For example consider a sample 3-bus network in Fig. 2 [2], for which (12) can be written as follows.

$$\begin{bmatrix} 1 & 0 & 0 & 0 & 0 \\ 0 & 1 & 0 & -E_2 & 0 \\ 0 & 0 & 1 & 0 & -E_3 \\ \mathbf{Z}_{12}^{-1} & -\mathbf{Z}_{12}^{-1} & 0 & 0 & 0 \\ -\mathbf{Z}_{13}^{-1} & 0 & \mathbf{Z}_{13}^{-1} & 0 & -\mathbf{I}_{31}^{local} \\ -\mathbf{Z}_{12}^{-1} & \mathbf{Z}_{12}^{-1} + \mathbf{Z}_{13}^{-1} & -\mathbf{Z}_{13}^{-1} & -\mathbf{I}_{2,inj}^{local} & 0 \end{bmatrix} \begin{bmatrix} E_1 \\ E_2 \\ E_3 \\ e^{j\hat{\delta}_2} \\ e^{j\hat{\delta}_3} \end{bmatrix} = \mathbf{I}_{12}^{local} \begin{bmatrix} E_1 \\ 0 \\ 0 \\ 0 \\ 0 \end{bmatrix} \quad (20)$$

It can be seen that in contrast to previous SE formulations, the one proposed here is exact and linear. It should be noted that, as opposed to those used in [20], the local currents in (20) are not synchrophasor measurements, but current phasors calculated from the corresponding voltage amplitude and power flow measurements. For example, \mathbf{I}_{31}^{local} can be calculated from the corresponding voltage amplitude and active and reactive power measurements as

$$\mathbf{I}_{31}^{local} = \frac{P_{31} - jQ_{31}}{E_3} \quad (21)$$

where all of the parameters in the right-hand side are SCADA measurements. Or alternately

$$\mathbf{I}_{31}^{local} = I_{31} e^{jtg^{-1}\left(-\frac{Q_{31}}{P_{31}}\right)} \quad (22)$$

where I_{31} is the current amplitude measurement [32], [33] provided by RTU at bus 3. It is worth noting that we have assumed current amplitude measurements are available. Therefore, there is no need for voltage amplitude measurements to calculate current phasors (see (22)). If current amplitude measurements are unavailable, then a noisy voltage measurements translates into the noisy current phasor in (21) (see also (29)), which is handled by the LS estimation. If a voltage measurement suffers gross error, this error propagates to different current phasors relating to the same bus. Smearing and masking effect [37] is

probable in this scenario, and typical bad data identifiers (e.g. largest normalized residual test) may fail. However, 1) with the existing communication network, it is not a heavy burden to send I_{ab}^{meas} , and, therefore this problem can be avoided; 2) this situation impacts also conventional SE; 3) if current amplitude measurements are not available, a two-level SE [16] may be employed where redundant voltage measurements by different IEDs are used to reject erroneous voltage measurement at substation-level SE.

V. MINIMUM-VARIANCE COMPLEX STATE ESTIMATION

Once phase angles of complex voltages at all buses are calculated from (19), it is possible to formulate the problem as a linear minimum-variance estimation. This is achieved by putting all the voltage and current measurements in the measurement vector as shown in (23) at the bottom of next page. Assuming that the voltage and current measurement errors have Gaussian distributions, according to (A.4) we can write (23) in a compact form as

$$\mathbf{T}\mathbf{y} + \mathbf{e} = \mathbf{m} \quad (24)$$

where $\mathbf{y} = [\mathbf{E}_1 \mathbf{E}_2 \dots \mathbf{E}_n]^T$ is the complex state vector and \mathbf{m} consists of voltage and current measurements. Following the procedure in Appendix A, the minimum-variance estimate of \mathbf{y} is given by

$$\hat{\mathbf{y}} = (\mathbf{T}^* R^{-1} \mathbf{T})^{-1} \mathbf{T}^* R^{-1} \mathbf{m} \quad (25)$$

where R is the diagonal covariance matrix of measurements, consisting of standard deviations of voltage, current and phase-angle measurements as follows (See Appendix A).

$$R_{ii} = \begin{cases} \sigma_{E_i}^2 & i'th \text{ voltage measurement} \\ \sigma_{I_{ab}}^2 + \sigma_{\theta_{ab}}^2 I_{ab}^{meas^2} & i'th \text{ current measurement} \end{cases} \quad (26)$$

In deriving (26), the time skew between measurements has been neglected, although in practice different measurements across the grid are not time-aligned. However, under normal operating conditions, the system state is assumed to remain unchanged during a few seconds before the measurements get updated, and therefore R is assumed diagonal [2], [3]. Moreover, since δ_i values are estimated by a large number of measurements, it has been assumed that they have much smaller standard deviations compared to $\sigma_{\theta_{ab}}$ in (26). Typical results from simulations presented in later show that this is practically true. For the 3-bus network in Fig. 2, the system of equations in the second stage can be written as follows

$$\begin{bmatrix} 1 & 0 & 0 \\ 0 & 1 & 0 \\ 0 & 0 & 1 \\ \mathbf{Z}_{12}^{-1} & -\mathbf{Z}_{12}^{-1} & 0 \\ -\mathbf{Z}_{13}^{-1} & 0 & \mathbf{Z}_{13}^{-1} \\ -\mathbf{Z}_{12}^{-1} & \mathbf{Z}_{12}^{-1} + \mathbf{Z}_{13}^{-1} & -\mathbf{Z}_{13}^{-1} \end{bmatrix} \begin{bmatrix} E_1 \\ E_2 \\ E_3 \\ \mathbf{I}_{12}^{local} \\ \mathbf{I}_{31}^{local} \\ \mathbf{I}_{2,inj}^{local} \end{bmatrix} = \begin{bmatrix} E_1 \\ E_2 e^{j\hat{\delta}_2} \\ E_3 e^{j\hat{\delta}_3} \\ \mathbf{I}_{12}^{local} \\ \mathbf{I}_{31}^{local} e^{j\hat{\delta}_3} \\ \mathbf{I}_{2,inj}^{local} e^{j\hat{\delta}_2} \end{bmatrix} \quad (27)$$

where $\hat{\delta}_2$ and $\hat{\delta}_3$ were estimated by (20) in the first stage. Therefore, $\hat{\delta}_2$ and $\hat{\delta}_3$ in (27) do not equal their true values due to the measurement noise. However, they play the same role as noisy measurements in conventional SE.

VI. CASE STUDIES

A. IEEE 118-bus Test System

In this part, the accuracy of the proposed complex linear SE algorithm is analyzed. In all simulations, the standard deviation of current amplitude and power flow measurements are assumed to be two times that of voltage amplitude measurements, unless stated otherwise. The step-by-step algorithm for simulations are as follows.

1. Run a load flow.
2. For bus a , receive voltage magnitude (E_a), active and reactive power flows through each line connected to bus a (P_{ab} , Q_{ab}) and current amplitude (I_{ab}).
3. Simulate voltage amplitude measurements by (11).
4. Simulate local current measurements. This is done by (1)-(4), where Gaussian error is added to construct input data from RTUs:

$$\mathbf{I}_{ab}^{local} = [I_{ab} + e_{I_{ab}}] e^{jtg^{-1}\left(-\frac{Q_{ab} + e_{Q_{ab}}}{P_{ab} + e_{P_{ab}}}\right)} \quad (28)$$

where $e_{I_{ab}}$, $e_{P_{ab}}$ and $e_{Q_{ab}}$ are zero-mean Gaussian random variables with corresponding variances to model measurement noise and I_{ab} , P_{ab} and Q_{ab} are obtained from load flow output. If the current amplitude measurement is not available then the local current measurement can be calculated by

$$\mathbf{I}_{ab}^{local} = \frac{P_{ab} + e_{P_{ab}} - j(Q_{ab} + e_{Q_{ab}})}{|E_a + e_{E_a}|} \quad (29)$$

When it comes to SCADA inputs from a substation RTU there are the following options:

- Option 1: P_{ab} , Q_{ab} , I_{ab} and E_a measurements are available.
- Option 2: P_{ab} , Q_{ab} and E_a measurements are available.

In the case of Option 1, the current phasors are calculated using (28). In the case of Option 2, the current phasors are calculated using (29).

We are assuming Option 1 in this paper. The reason is that Watt and VAR transducer errors, when obtaining P_{ab} and Q_{ab} by E_a and I_{ab} measurements, can be avoided.

The effect of redundancy and accuracy of measurements are analyzed for the IEEE 118-bus test system, and the convergence speed will be tested for 300-, 1341- and 9241-bus systems as well.

Fig. 3 visualizes the sparsity pattern of \mathbf{H} in the left-hand side of (13) for the 118-bus test system. Referring to (12), the pattern may be analyzed by the first 118 voltage measurements, last 118 injection measurements and current measurements in between. Fig. 4 shows the partitions \mathbf{A} , \mathbf{B} , \mathbf{C} and \mathbf{D} in (15). The diagonal matrix \mathbf{D} can easily be identified in this figure, which is useful in applying (19).

1) *Impact of Measurement Accuracy*: Different accuracy classes for measurements are considered in this part. It is assumed that voltage magnitudes at all buses, current measurements at both terminals of lines and current injections at all load and generator buses are measured. Standard deviations of complex voltage amplitude and phase-angle values from those of the true values are used as performance index (PI). The PI for voltage amplitude estimation is defined as follows.

$$\sigma_E = \frac{\sum_{a=1}^n |E_a^{est} - E_a^{true}|}{n} \quad (30)$$

where E_a^{est} and E_a^{true} are the estimated and exact voltage amplitude at bus a , respectively, and σ_E is the Mean Estimation Error (MEE) for bus voltage magnitude. Likewise, for phase angle of complex voltages, σ_δ is defined as

$$\sigma_\delta = \frac{\sum_{a=2}^n |\delta_a^{est} - \delta_a^{true}|}{n-1} \quad (31)$$

$$\begin{bmatrix} 1 & 0 & \dots & 0 \\ 0 & -1 & \dots & 0 \\ \vdots & \vdots & \vdots & \vdots \\ 0 & 0 & \dots & -1 \\ \mathbf{Y}_{12} + \mathbf{Z}_{12}^{-1} & -\mathbf{Z}_{12}^{-1} & 0 & 0 \\ 0 & \mathbf{Y}_{2n} + \mathbf{Z}_{2n}^{-1} & \dots & -\mathbf{Z}_{2n}^{-1} \\ \vdots & \vdots & \vdots & \vdots \\ 0 & -\mathbf{Z}_{n2}^{-1} & 0 & \mathbf{Y}_{n2} + \mathbf{Z}_{n2}^{-1} \\ -\mathbf{Z}_{n1}^{-1} & 0 & 0 & \mathbf{Y}_{n1} + \mathbf{Z}_{n1}^{-1} \\ \mathbf{Y}_{12} + \mathbf{Z}_{12}^{-1} + \mathbf{Y}_{1n} + \mathbf{Z}_{1n}^{-1} & -\mathbf{Z}_{12}^{-1} & 0 & -\mathbf{Z}_{1n}^{-1} \\ -\mathbf{Z}_{21}^{-1} & \mathbf{Y}_{21} + \mathbf{Z}_{21}^{-1} + \mathbf{Y}_{2n} + \mathbf{Z}_{2n}^{-1} & 0 & -\mathbf{Z}_{2n}^{-1} \\ \vdots & \vdots & \vdots & \vdots \end{bmatrix} \begin{bmatrix} \mathbf{E}_1 \\ \mathbf{E}_2 \\ \vdots \\ \mathbf{E}_n \end{bmatrix} = \begin{bmatrix} E_1 \\ -E_2 e^{j\hat{\delta}_2} \\ \vdots \\ -E_n e^{j\hat{\delta}_n} \\ \mathbf{I}_{12}^{local} \\ \mathbf{I}_{2n}^{local} e^{j\hat{\delta}_2} \\ \vdots \\ \mathbf{I}_{n2}^{local} e^{j\hat{\delta}_n} \\ \mathbf{I}_{n1}^{local} e^{j\hat{\delta}_n} \\ \mathbf{I}_{1,inj}^{local} \\ \mathbf{I}_{2,inj}^{local} e^{j\hat{\delta}_2} \\ \vdots \end{bmatrix} \quad (23)$$

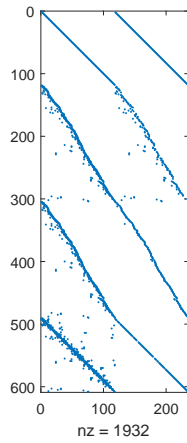


Figure 3. Visualization of H for the IEEE 118-Bus Test System (HR case).

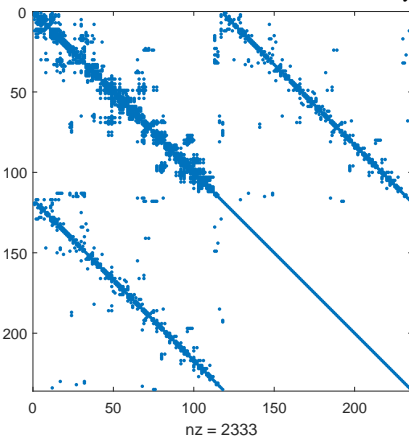


Figure 4. Visualization of (15) for the IEEE 118-Bus Test System.

Figs. 5 and 6 show the results of the linear SE for 1000 measurement sets, generated randomly from the exact load flow results. Three values for standard deviation of bus voltage measurements (σ) are considered randomly. As expected, the more the standard deviation of measurements, the more the standard deviation of estimated voltage magnitudes and phase angles. It can be seen from Fig. 5 that since various measurements contribute to the SE, the mean value for the standard deviation of estimated bus voltage magnitudes are less than that of the measurements. Moreover, accuracy of the estimated phase angles are mostly better than 0.3° even with the least accurate measurements, which can be considered most desirable for practical systems.

In order to confirm the effect of considering different accuracy levels for different measurements, Fig. 7 shows results for phase-angle estimates of a typical SE case. It can be observed that although LS estimation in the first step (Section IV) yields acceptable estimates for phase angles, the WLS estimation in the second step (Section V) has improved the phase angle estimates by incorporating different accuracy levels of measurements.

2) *Impact of Measurement Redundancy*: Two cases of low and high redundancy of measurements are studied in this part. The low redundancy (LR) case consists of voltage

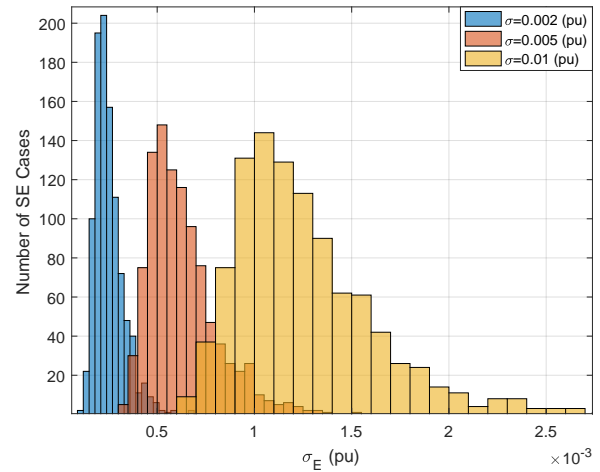


Figure 5. Impact of measurement accuracy on voltage magnitude estimation.

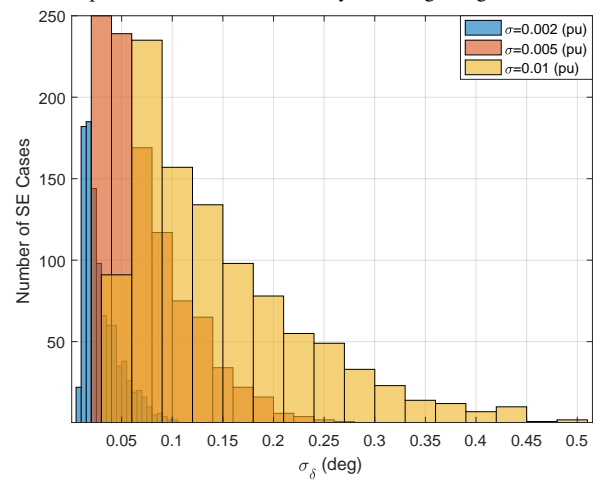


Figure 6. Impact of measurement accuracy on voltage phase-angle estimation.

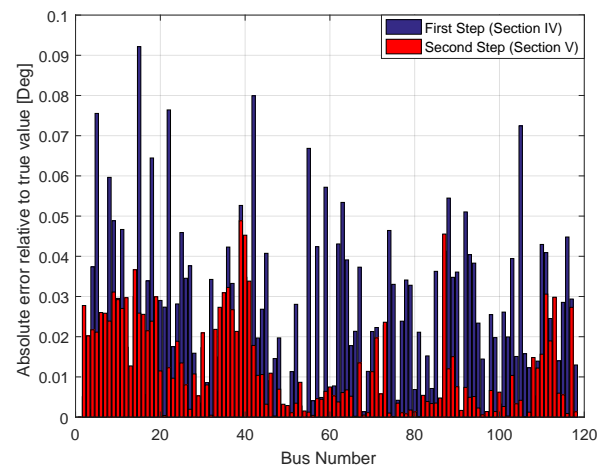


Figure 7. Comparison between LS and WLS SE for phase-angle estimation.

measurement at all buses, injection measurements at half of the buses (buses 1, 3, ...) and current measurements at one terminal of every line ("from" terminal in the MATPOWER format [38]). High redundancy (HR) case includes injection measurements at all buses and current measurement at both terminals of every line, together with voltage measurements at all buses. Table I shows the average MEE of complex

Table I
IMPACT OF MEASUREMENT REDUNDANCY ON STATE ESTIMATION.

Case	$\bar{\sigma}_E(pu)$	$\bar{\sigma}_\delta(deg)$
High Redundancy	2.52e-4	2.98e-2
Low Redundancy	3.18e-4	3.1e-2

Table II
COMPARISON BETWEEN PROPOSED AND CONVENTIONAL METHODS FOR STATE ESTIMATION

Case	$\bar{\sigma}_E(pu)$	$\bar{\sigma}_\delta(deg)$
Proposed Method	2.52e-4	2.98e-2
Conventional Method	1.17e-3	2.84e-2

Table III
BAD DATA DETECTION AND IDENTIFICATION FOR ERRONEOUS MEASUREMENT I_{26-30}

Measurement	True Value	Measured Value	Normalized Residual
I_{26-30}	2.2385	1.1206	104.6
$I_{30,in,j}$	0	0.0031	38.9
$I_{26,in,j}$	3.3496	3.3521	20.1
I_{8-30}	0.745	0.7357	17.9

voltage amplitude and phase angle obtained under LR and HR of measurements by conducting 1000 simulation cases. As expected and confirmed by the obtained results, the higher the redundancy of measurements, the more accurate the SE results.

3) *Comparison with Conventional SE:* Conventionally, an iterative method based on Gauss-Newton algorithm has been adopted to solve the SE problem. To make a comparison between the conventional and the proposed methods, 1000 Monte-Carlo simulations have been carried out on the 118-bus test system. For the conventional SE, *run_se.m* and *doSE.m* in MATPOWER [38] have been modified to include injection measurements at all buses and initialize voltages according to measured voltage magnitudes in flat start. The standard deviation for voltage and power measurements (active and reactive) have been set to 0.2 % and 0.4%, respectively, similar to the proposed method. Table II reflects the results for the average of performance indices over 1000 simulation cases. It is evident that the proposed method outperforms the iterative-based conventional method in term of accuracy of the estimation.

4) *Bad Data Identification:* Largest Normalized Residual Test (LNRT) may be utilized to detect and identify bad data in order to improve the SE results [2]. In order to evaluate LNRT for the IEEE 118-bus test system, various measurement errors in different HR and LR conditions have been carried out, successfully. AS an example, in LR condition, the current measurement through the 345-kV line 26-30 is halved in order to simulate bad data. Table III shows the LNRT result for four measurements with the largest large normalized residuals where the bad data is identified, correctly.

Table IV
COMPUTATION TIME OF STATE ESTIMATION (IN SECONDS) FOR DIFFERENT SYSTEMS

System	Semidefinite Programming [9]	Complex Linear
9-bus	1.58	0.0019
14-bus	2.54	0.0032
30-bus	3.21	0.0066
57-bus	4.09	0.0156
118-bus	5.63	0.0558
1354-bus	9.48	0.1428
9241-bus	109.14	1.3044

B. 1354- and 9241-bus Pan-European High-Voltage Grids

Figs. 8 and 9 compare the SE performance indexes for different systems from 118 to 9241 buses. One can conclude that the system size does not significantly impact the performance of the linear SE method. Even on large-scale systems, the implementation of SE is ultra fast. Table IV compares the solution time for systems of different sizes. All simulations for the proposed linear SE are carried out by a PC with Core i7 6500U CPU at 2.5 GHz and 16 GB of RAM. It should be noted that the results for the SDP-based approach are directly reported from [9], where for the last two systems a macOS system with 2.2 GHz CPU and 12 GB RAM was used while a Windows system with 2.7 GHz CPU and 8GB RAM was utilized for other systems. Computation time for [23] as a complex but iteration-based method has also been reported directly in Table V and compared with the proposed method. It should be noted that less measurements are used in SE problem for Table V compared with Table IV, hence less computation time for the proposed method in the former table. Even though the Core i5-6600k CPU used in [23] is twice as fast as ours [39], the proposed linear SE algorithm outperforms the complex iterative algorithm in [23], which needs 5 iterations to solve SE for the 9241-bus system.

Moreover, in contrast to the proposed algorithm, the algorithm in [23] needs PMU measurements to solve SE, a requirement not imposed on the proposed algorithm. Furthermore, the matrices used in the proposed method comprise mostly of constant parameters of the system, therefore need to be built once and updated slightly based on network topology changes.

Simulation results indicate fast speed of the proposed complex linear method, since it only requires solving a linear system of equations. This has resulted in fast solution of SE for different systems, especially almost 1 second and 0.25 second for the 9241-bus system in high and low redundancy of measurements, respectively.

VII. CONCLUSION

A complex linear formulation of the SE problem, utilizing unsynchronized RTU measurements, has been presented in this paper. In contrast to the conventional SE currently used in modern EMS in control rooms, the proposed method does

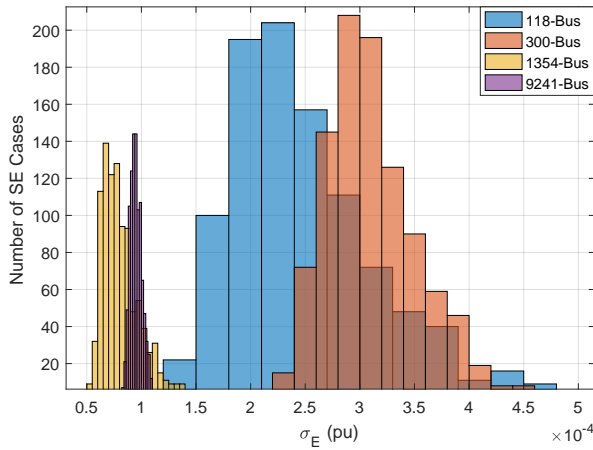


Figure 8. Comparison of estimated voltage magnitude for different systems.

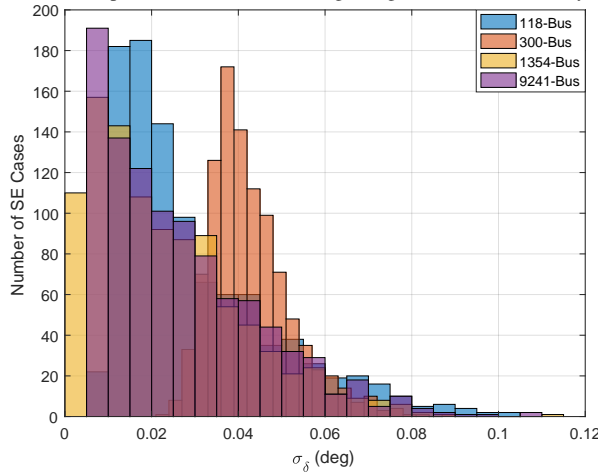


Figure 9. Comparison of estimated voltage phase angle for different systems.

Table V
COMPARISON BETWEEN COMPLEX ITERATIVE [23] AND PROPOSED COMPLEX LINEAR ALGORITHMS

System	Complex Iterative [23]	Complex Linear
118-bus	1.2 ms	4.7 ms
9241-bus	312.7 ms	243.1 ms
CPU Speed Rank [39]	38 th /1103	349 th /1103

not need initialization, involves no iterations, and is solved swiftly with no concern about convergence. The first property is quite useful in operating conditions when initialization in the conventional SE may move apart from the current system state. The other properties mentioned above make SE feasible for large-scale grids with detailed models at different voltage levels. As much as SE needs to be solved regularly enough, the present iterative methods based on SCADA measurements are too slow to implement on large-scale models. Utilizing the same measurements, the proposed method, in contrast, is carried out ultra fast, taking almost one second even for the large-scale 9241-bus Pan-European grid. The proposed method has been tested on several systems including 6 up to nearly 10,000 buses, where results confirm that it outperforms the conventional algorithm in terms of solution speed.

APPENDIX A COMPLEX LINEAR LEAST SQUARES

Consider a complex random variable $\mathbf{z}_i = z_i e^{j\delta_i}$ defined by two real-valued random variables $z_i \sim \mathcal{N}(z_i^{true}, \sigma_{z_i}^2)$ and $\delta_i \sim \mathcal{N}(\delta_i^{true}, \sigma_{\delta_i}^2)$, which are independent. Therefore \mathbf{z}_i can be written as

$$z_i e^{j\delta_i} = (z_i^{true} + e_{z_i}) e^{j(\delta_i^{true} + e_{\delta_i})} \quad (A.1)$$

where $e_{z_i} \sim \mathcal{N}(0, \sigma_{z_i}^2)$ and $e_{\delta_i} \sim \mathcal{N}(0, \sigma_{\delta_i}^2)$ are independent measurement errors of magnitude and phase angle of \mathbf{z}_i , respectively. Taylor series expansion of $e^{j\delta_i}$ is written as

$$e^{j\delta_i} = 1 + j e_{\delta_i} - \frac{e_{\delta_i}^2}{2} + \dots \quad (A.2)$$

Assuming small phase-angle error, the higher order terms in (A.2) may be neglected. Substituting $e^{j\delta_i} = 1 + j e_{\delta_i}$ into (A.1) we have:

$$\mathbf{z}_i = \mathbf{z}_i^{true} + e_{z_i} e^{j\delta_i^{true}} + j e_{\delta_i} \mathbf{z}_i^{true} \quad (A.3)$$

where $\mathbf{z}_i^{true} = z_i^{true} e^{j\delta_i^{true}}$ is the complex true value of \mathbf{z}_i and is never known due to statistical nature of measurement errors. Now consider complex vector \mathbf{z} containing m complex measurements related to the complex state \mathbf{x} linearly. That is

$$\mathbf{z} = \mathbf{H}\mathbf{x} + \mathbf{e} \quad (A.4)$$

where \mathbf{H} is the constant complex coefficient matrix, \mathbf{x} is the complex state vector and \mathbf{e} is the complex error vector. According to (A.3) the i th element of \mathbf{e} , designated as e_i , may be written as

$$e_i = e_{z_i} e^{j\delta_i^{true}} + j e_{\delta_i} z_i^{true} = e^{j\delta_i^{true}} (e_{z_i} + j e_{\delta_i} z_i^{true}) \quad (A.5)$$

The minimum-variance estimation of \mathbf{x} in (A.4) is obtained by solving the following least squares formulation [40].

$$\underset{\mathbf{x}}{\text{Min}} \quad \mathbf{e}^* \mathbf{R}^{-1} \mathbf{e} = (\mathbf{z} - \mathbf{H}\mathbf{x})^* \mathbf{R}^{-1} (\mathbf{z} - \mathbf{H}\mathbf{x}) \quad (A.6)$$

where $\mathbf{R} = \mathbb{E}(\mathbf{e}\mathbf{e}^*)$ is the complex covariance matrix of measurement errors. The best linear unbiased estimate of \mathbf{x} is given by [40]:

$$\hat{\mathbf{x}} = (\mathbf{H}^* \mathbf{R}^{-1} \mathbf{H})^{-1} \mathbf{H}^* \mathbf{R}^{-1} \mathbf{z} \quad (A.7)$$

If measurement errors are assumed to be independent, the covariance matrix \mathbf{R} in (A.6)-(A.7) will be real-valued and diagonal, whose elements are calculated according to (A.5) as

$$R_{ii} = \mathbb{E}(\mathbf{e}_i \mathbf{e}_i^*) = \mathbb{E}(|\mathbf{e}_i|^2) = \mathbb{E}(e_{z_i}^2 + e_{\delta_i}^2 z_i^{true^2}) \quad (A.8)$$

which can be expressed in terms of variances of magnitude and phase angle of the complex measurement as

$$R_{ii} = \sigma_{z_i}^2 + \sigma_{\delta_i}^2 z_i^{true^2} \quad (A.9)$$

REFERENCES

- [1] F. F. Wu, K. Moslehi, and A. Bose, "Power system control centers: Past, present, and future," *Proceedings of the IEEE*, vol. 93, no. 11, pp. 1890–1908, 2005.
- [2] A. Abur and A. G. Exposito, *Power system state estimation: theory and implementation*. CRC Press, 2004.
- [3] A. J. Wood and B. F. Wollenberg, *Power generation, operation, and control*. John Wiley & Sons, 2012.
- [4] Y.-F. Huang, S. Werner, J. Huang, N. Kashyap, and V. Gupta, "State estimation in electric power grids: Meeting new challenges presented by the requirements of the future grid," *IEEE Signal Processing Magazine*, vol. 29, no. 5, pp. 33–43, 2012.
- [5] Y. Weng, R. Negi, C. Faloutsos, and M. D. Ilić, "Robust data-driven state estimation for smart grid," *IEEE Trans. Smart Grid*, vol. 8, no. 4, pp. 1956 – 1967, 2017.
- [6] Y. Weng, Q. Li, R. Negi, and M. Ilić, "Semidefinite programming for power system state estimation," in *Power and Energy Society General Meeting, 2012 IEEE*. IEEE, 2012, pp. 1–8.
- [7] H. Zhu and G. B. Giannakis, "Power system nonlinear state estimation using distributed semidefinite programming," *IEEE Jour. Sel. Topics Signal Proc.*, vol. 8, no. 6, pp. 1039–1050, 2014.
- [8] R. Madani, M. Ashraphijuo, J. Lavaei, and R. Baldick, "Power system state estimation with a limited number of measurements," in *Decision and Control (CDC), 2016 IEEE 55th Conference on*. IEEE, 2016, pp. 672–679.
- [9] Y. Zhang, R. Madani, and J. Lavaei, "Conic relaxations for power system state estimation with line measurements," *IEEE Trans. Control Network Syst.*, 2017.
- [10] C. Gomez-Quiles, A. de la Villa Jaen, and A. Gomez-Exposito, "A factorized approach to wls state estimation," *IEEE Trans. Power Syst.*, vol. 26, no. 3, pp. 1724–1732, 2011.
- [11] A. Gomez-Exposito, C. Gomez-Quiles, and A. de la Villa Jaen, "Bilinear power system state estimation," *IEEE Trans. Power Syst.*, vol. 27, no. 1, pp. 493–501, 2012.
- [12] T. Wu, C. Chung, and I. Kamwa, "A fast state estimator for systems including limited number of pmus," *IEEE Trans. Power Syst.*, vol. 32, no. 6, pp. 4329–4339, 2017.
- [13] C. Gomez-Quiles, H. A. Gil, A. de la Villa Jaen, and A. Gomez-Exposito, "Equality-constrained bilinear state estimation," *IEEE Trans. Power Syst.*, vol. 28, no. 2, pp. 902–910, 2013.
- [14] R. Jabr and B. Pal, "AC network state estimation using linear measurement functions," *IET Gen., Transm. & Distrib.*, vol. 2, no. 1, pp. 1–6, 2008.
- [15] S. Chakrabarti, E. Kyriakides, T. Bi, D. Cai, and V. Terzija, "Measurements get together," *IEEE Power and Energy Magazine*, vol. 7, no. 1, 2009.
- [16] T. Yang, H. Sun, and A. Bose, "Transition to a two-level linear state estimator-part II: Algorithm," *IEEE Trans. Power Syst.*, vol. 26, no. 1, pp. 54–62, 2011.
- [17] M. Gol and A. Abur, "LAV based robust state estimation for systems measured by PMUs," *IEEE Trans. Smart Grid*, vol. 5, no. 4, pp. 1808–1814, 2014.
- [18] S. Sarri, L. Zanni, M. Popovic, J.-Y. Le Boudec, and M. Paolone, "Performance assessment of linear state estimators using synchrophasor measurements," *IEEE Trans. Instrum. Meas.*, vol. 65, no. 3, pp. 535–548, 2016.
- [19] L. Zhang, A. Bose, A. Jampala, V. Madani, and J. Giri, "Design, testing, and implementation of a linear state estimator in a real power system," *IEEE Trans. Smart Grid*, 2017.
- [20] J. Lin, Y. Su, Y. Cheng, C. Lu, L. Zhu, H. Huang, and Y. Liu, "A robust complex-domain state estimator using synchrophasor measurements," *Int. Jour. Electr. Power & Energy Syst.*, vol. 96, pp. 412–421, 2018.
- [21] G. Valverde, S. Chakrabarti, E. Kyriakides, and V. Terzija, "A constrained formulation for hybrid state estimation," *IEEE Trans. Power Syst.*, vol. 26, no. 3, pp. 1102–1109, 2011.
- [22] T. Bi, X. Qin, and Q. Yang, "A novel hybrid state estimator for including synchronized phasor measurements," *Electr. Power Syst. Res.*, vol. 78, no. 8, pp. 1343–1352, 2008.
- [23] I. Dzaifc, R. A. Jabr, and T. Hrnjic, "Hybrid state estimation in complex variables," *IEEE Trans. Power Syst.*, 2018.
- [24] B. Fardanesh, "Direct non-iterative power system state solution and estimation," in *Power and Energy Society General Meeting, 2012 IEEE*. IEEE, 2012, pp. 1–6.
- [25] X. T. Jiang, B. Fardanesh, D. Maragal, G. Stefopoulos, J. H. Chow, and M. Razanousky, "Improving performance of the non-iterative direct state estimation method," in *Power and Energy Conference at Illinois (PECI), 2014*. IEEE, 2014, pp. 1–6.
- [26] X. T. Jiang, J. H. Chow, B. Fardanesh, D. Maragal, G. Stefopoulos, and M. Razanousky, "Power system state estimation using a direct non-iterative method," *Int. Jour. Electr. Power & Energy Syst.*, vol. 73, pp. 361–368, 2015.
- [27] F. C. Schweppe, "Power system static-state estimation, part iii: Implementation," *IEEE Trans. Power App. syst.*, no. 1, pp. 130–135, 1970.
- [28] J. R. Gilbert, C. Moler, and R. Schreiber, "Sparse matrices in MATLAB: Design and implementation," *SIAM Journal on Matrix Analysis and Applications*, vol. 13, no. 1, pp. 333–356, 1992.
- [29] E. Ghahremani and I. Kamwa, "Dynamic state estimation in power system by applying the extended kalman filter with unknown inputs to phasor measurements," *IEEE Trans. Power Syst.*, vol. 26, no. 4, pp. 2556–2566, 2011.
- [30] T. D. Mohanadhas, N. Sarma, and T. Mortensen, "State estimation performance monitoring at ERCOT," in *Power Systems Conference (NPSC), 2016 National*. IEEE, 2016, pp. 1–6.
- [31] State estimation performance monitoring. [Online]. Available: https://www.nerc.com/pa/trm/resources/monitoring_and_situational_awareness_conference/1/10.%20monitoring%20se%20performance%20at%20ercot_sarma%20nuthalapati_ercot.pdf
- [32] RTU3200 product data sheet. [Online]. Available: http://www.clevelandprice.com/wp-content/uploads/2017/01/RTU3200_DataSheet.pdf
- [33] A. Monticelli, *State estimation in electric power systems: a generalized approach*. Springer Science & Business Media, 2012.
- [34] ABB state estimation. [Online]. Available: <https://library.e.abb.com/public/7ea594006f544abfc1257b0c0055220f/State%20Estimation.pdf>
- [35] Siemens network applications solutions, state estimation. [Online]. Available: https://www.energy.siemens.com/mx/pool/hq/services/power-transmission-distribution/power-technologies-international/software-solutions/pss-odms/Network_Applications.pdf
- [36] D. S. Bernstein, *Matrix mathematics: theory, facts, and formulas*. Princeton University Press, 2009.
- [37] T. Van Cutsem, M. Ribbens-Pavella, and L. Mili, "Bad data identification methods in power system state estimation-a comparative study," *IEEE Tans. Power App. Syst.*, no. 11, pp. 3037–3049, 1985.
- [38] Matpower: A matlab power system simulation package. [Online]. Available: <http://www.pserc.cornell.edu/matpower/>
- [39] CPU benchmark. [Online]. Available: <http://cpu.userbenchmark.com/Compare/Intel-Core-i7-6500U-vs-Intel-Core-i5-6600K/m36930vs3503>
- [40] K. S. Miller, "Complex linear least squares," *SIAM Review*, vol. 15, no. 4, pp. 706–726, 1973.